Increasing the RES Hosting Capacity in Distribution Systems Through Reconfiguration with Closed-Loop Operation and Voltage Control

Juan M. Home-Ortiz
Department of Electrical Engineering
São Paulo State University
Ilha Solteira, Brazil
juan.home@unesp.br

Leonardo H. Macedo
Department of Electrical Engineering
São Paulo State University
Ilha Solteira, Brazil
leohfmp@ieee.org

Renzo Vargas
Engineering, Modeling and Applied Social Sciences Center
Federal University of ABC–UFABC
Santo André, Brazil
renzo@ieee.org

Rubén Romero
Department of Electrical Engineering
São Paulo State University
Ilha Solteira, Brazil
ruben.romero@unesp.br

José Roberto Sanches Mantovani
Department of Electrical Engineering
São Paulo State University
Ilha Solteira, Brazil
mant@dee.feis.unesp.br

João P. S. Catalão
FEUP and INESC TEC
Porto, Portugal
catalao@fe.up.pt

2021 International Conference on Smart Energy Systems and Technologies (SEST) | 978-1-7281-7660-4/21/$31.00 ©2021 IEEE | DOI: 10.1109/SEST50973.2021.9543318

***Abstract*—This paper presents a novel mixed-integer second-order cone programming model to increase the photovoltaic (PV) hosting capacity and optimize the operation of distribution systems. The operational problem considers voltage control through the optimal operation of capacitors banks, substations' on-load tap changers, voltage regulators, and network reconfiguration with radial and closed-loop operation. The proposed formulation considers voltage-dependent models for loads and capacitor banks. The objective function maximizes the PV hosting capacity of the system. Numerical experiments are carried out using the 33-node system and results demonstrate the effectiveness of the proposed formulation to increase the penetration of PV sources, especially when the closed-loop operation is allowed, together with network reconfiguration.**

Keywords—Closed-loop topology, distribution systems reconfiguration, mixed-integer second-order cone programming, PV hosting capacity, voltage-dependent models.

NOMENCLATURE

Indices and sets:

i, j	Indices for nodes
ij, ji	Indices for branches
k	Index for capacitor banks' (CBs) modules
s	Index for stochastic scenarios
Γ_B	Set of branches
Γ_{CB}	Set of nodes with capacitor banks
Γ_{DG}	Set of nodes with dispatchable distributed generators (DGs)
Γ_N	Set of nodes
Γ_{PV}	Set of candidate nodes to install PV generation
Γ_S	Set of stochastic scenarios
Γ_{SS}	Set of substations (SSs) nodes
Γ_{TC}	Set of branches with voltage regulators (VRs)/SSs' on-load tap changers (OLTCs)

Parameters:

B_i^{CB}	Susceptance of a CB's module installed at a node
$e_{i,s}^{DG}, e_{i,s}^{SS}$	CO_2 emissions intensity for dispatchable DGs and SSs
$\overline{I}_{ij}$	Current capacity of a branch
M^V, M^Θ	Big-M parameters
N^{LP}	Maximum number of basic loops allowed to be formed in the system
$P_{i,s}^D, Q_{i,s}^D$	Active/reactive power load at nominal voltage
$\underline{PF}_i^{DG}, \overline{PF}_i^{DG}$	Power factor limits of a dispatchable DG
$\underline{PF}_i^{PV}, \overline{PF}_i^{PV}$	Power factor limits of a PV unit
R_{ij}, X_{ij}, Z_{ij}	Resistance, reactance, and impedance of a branch
$\overline{S}_i^{DG}$	Apparent power capacity of a dispatchable DG
$\overline{S}_i^{SS}$	Apparent power capacity of a SS
$\overline{V}, \underline{V}$	Maximum/minimum voltage magnitude limits
V^N	Nominal voltage of the system
$\overline{n}_i^{CB}$	Number of CB's modules installed at a node
$\hat{v}_{i,s}$	Estimate of the voltage magnitude
Δ_s^T	Duration of a stochastic scenario
$\overline{\Delta}_{ij}^{TC}$	Regulation of a VR/SS's OLTC
$\gamma_{i,s}^Z, \gamma_{i,s}^I, \gamma_{i,s}^P$	Participation factors of constant impedance/current/power of the active power demand
$\lambda_{i,s}^{PV}$	Generation factor of a PV generation unit
$\mu_{i,s}^Z, \mu_{i,s}^I, \mu_{i,s}^P$	Participation factors of constant impedance/current/power of the reactive power demand
ξ	Total CO_2 emissions from the system
ψ_i	Power curtailment limit for a PV unit

Continuous variables:

$I_{ij,s}^{SQ}$	Square of the current magnitude on a branch
$P_{ij,s}, Q_{ij,s}$	Active/reactive power flows through a branch
$P_{i,s}^C$	Power curtailment for a PV generation unit
$P_{i,s}^{DG}, Q_{i,s}^{DG}$	Active/reactive power injected by a DG
$P_{i,s}^{PV}, Q_{i,s}^{PV}$	Active/reactive power injected by a PV generator
$\overline{P}_i^{PV}$	Installed PV capacity
$P_{i,s}^{SS}, Q_{i,s}^{SS}$	Active/reactive power injected by a SS
$Q_{i,k,s}^{CB}$	Reactive power injected by a CB's module
$\hat{Q}_{i,s}^{CB}$	Total reactive power injected by a CB
$V_{i,s}$	Voltage magnitude at a node
$V_{i,s}^{SQ}$	Square of the voltage magnitude at a node
f_{ij}	Fictitious flow on a branch
g_i	Fictitious generation at SS nodes
$\delta_{ij,s}^{TC}$	Auxiliary variable for voltage regulators
$\zeta_{ij,s}, \xi_{ij,s}$	Slack variables for the calculation of the voltage drop/angle difference across a branch
$\theta_{i,s}$	Voltage angle at a node

Binary variables:

w_{ij}^{SW}	Operational state of a branch
$y_{i,k,s}^{CB}$	Indicates if a CB module is operating or not

978-1-7281-7660-4/21/$31.00 ©2021 IEEE

I. Introduction

Environmental concerns have incentivized the inclusion of renewable energy sources (RES) in electrical distribution networks. Encouraged by governmental incentives [1], CO_2 emissions mitigation strategies [2], reduction of electricity bills [3], and a continuous decrease in equipment costs [4], the presence of RES in distribution systems has increased over the years.

However, the introduction of these technologies in electric grids brings new challenges for the operational planners due to RES generation characteristics. These characteristics include an intermittent behavior, which has an impact on the voltage and current constraints of the networks [5], [6]. These impacts could limit the amount of RES insertion in distribution networks and could only be mitigated through investments to reinforce the network. As such, the operational planners look for alternatives to adequate and improve the operation of distribution systems in order to include more RES in the network.

Network reconfiguration is one of the most common approaches to improve the operation of distribution systems. It consists of performing switching operations with the objective of changing the topology of the network for alleviating congestions and improving the voltage profile while maintaining a radial configuration for the system. Reference [7] evaluates the possibility of performing network reconfiguration for improving the hosting capacity of distribution networks maintaining a radial configuration. In [8], the authors formulate a network reconfiguration problem to minimize voltage violations associated with increasing PV penetration in a radial distribution system.

Closed-loop operation topology is an alternative for radial operation in distribution networks. The advantages of a closed-loop operation include a potential decrease of electric losses [9] and reliability improvements in the normal state [10]. On the other hand, in contingency scenarios, the response of the system after a permanent fault is enhanced by reconnecting more loads to primary feeders [11]. In [9], the reconfiguration problem considering the closed-loop operation for minimizing electric losses is formulated as a mixed-integer nonlinear programming (MINLP) problem. A very important aspect of this work is that the authors verify that not necessarily an all-closed-switches operation configuration is the topology with lower power losses. In [12], the possibility of considering a closed-loop operation topology of the network for improving the integration of RES in distribution systems is analyzed, considering only the possibility of closing tie switches, i.e., without considering network reconfiguration.

Voltage control is another option to improve the operation of distribution systems. It consists of determining the optimal adjustment of the tap positions of the substations' (SSs) on-load tap changers (OLTCs), voltage regulators (VRs), and the determination of the number of capacitor banks (CBs) in operation at each node. Reference [13] proposes a mathematical formulation to improve the hosting capacity of active distribution networks through voltage control without changing the network topology.

In this work, we consider network reconfiguration, voltage control, and closed-loop operation for increasing the maximum penetration of RES in distribution systems. Differently from [12], the proposed approach considers opening sectionalizing switches to provide more flexibility to the network operation. The proposed formulation consists of a new mixed-integer second-order cone programming (MISOCP) model. To handle the uncertainties of RES, a stochastic scenario-based formulation is used. The load is represented using the voltage-dependent ZIP model to characterize a more realistic representation of the problem. The objective function considers the maximization of the penetration of RES in the distribution systems in order to mitigate CO_2 emissions. Tests are performed using a 33-node distribution system.

The main contributions of this work are as follows:

- From a modeling perspective, a new stochastic-programming-based model is proposed to determine the optimal distribution network topology, allowing closed-loop operation and voltage control, in order to increase the PV hosting capacity of the system and reduce the associated CO_2 emissions;
- From a methodological perspective, the resulting MINLP problem is recast in order to obtain a relaxed MISOCP model that is treatable, scalable, and can be effectively solved by commercial solvers.

The remainder of the paper is organized as follows: Section II presents the proposed formulation for the problem; the results of the tests conducted using the 33-node system are presented in Section III; finally, the conclusions of the work are presented in Section IV.

II. Problem Formulation

A. Objective Function

The formulation maximizes the PV hosting capacity of the system. Equation (1) presents the objective function $\mathcal{F}$ of the problem.

$$\text{maximize}\,\mathcal{F} = \sum_{i\in\Gamma_{PV}} \overline{P}_i^{PV} \tag{1}$$

In (1), the sum of the PV generation installed capacity at each node i is maximized.

B. Power Flow Constraints

The ac operation of the system is represented by the power flow equations (2)–(9) [11].

$$\sum_{ji\in\Gamma_B} P_{ji,s} - \sum_{ij\in\Gamma_B}\left(P_{ij,s} + R_{ij}I_{ij,s}^{SQ}\right) + P_{i,s}^{SS} + P_{i,s}^{DG} + P_{i,s}^{PV} = P_{i,s}^{D}\left[\gamma_{i,s}^{Z}\frac{V_{i,s}^{SQ}}{(V^N)^2} + \gamma_{i,s}^{I}\frac{V_{i,s}}{V^N} + \gamma_{i,s}^{P}\right] \tag{2}$$

$$\sum_{ji\in\Gamma_B} Q_{ji,s} - \sum_{ij\in\Gamma_B}\left(Q_{ij,s} + X_{ij}I_{ij,s}^{SQ}\right) + Q_{i,s}^{SS} + Q_{i,s}^{DG} + Q_{i,s}^{PV} + \hat{Q}_{i,s}^{CB} = Q_{i,s}^{D}\left[\mu_{i,s}^{Z}\frac{V_{i,s}^{SQ}}{(V^N)^2} + \mu_{i,s}^{I}\frac{V_{i,s}}{V^N} + \mu_{i,s}^{P}\right] \tag{3}$$

$$V_{i,s} = \sqrt{\frac{\overline{V}+\underline{V}}{2}} + \frac{1}{2\sqrt{\frac{\overline{V}+\underline{V}}{2}}}\left(V_{i,s}^{SQ} - \frac{\overline{V}+\underline{V}}{2}\right) \tag{4}$$

$$\forall i \in \Gamma_N, s \in \Gamma_S$$

$$V_{i,s}^{SQ} - V_{j,s}^{SQ} + \delta_{ij,s}^{TC} + \zeta_{ij,s} = 2(R_{ij}P_{ij,s} + X_{ij}Q_{ij,s}) + Z_{ij}^2 I_{ij,s}^{SQ} \tag{5}$$

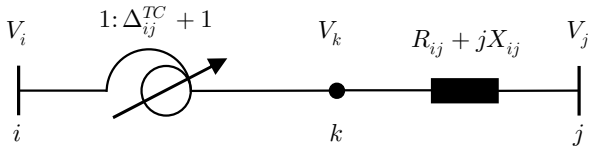

Fig. 1 Equivalent circuit of a VR/SS's OLTC.

$$\hat{v}_{i,s}\hat{v}_{j,s}(\theta_{i,s}-\theta_{j,s}+\xi_{ij,s}) = X_{ij}P_{ij,s} - R_{ij}Q_{ij,s} \tag{6}$$

$$V_{j,s}^{SQ} I_{ij,s}^{SQ} \geq P_{ij,s}^2 + Q_{ij,s}^2 \tag{7}$$

$$|\zeta_{ij,s}| \leq M^V(1-w_{ij}^{SW}) \tag{8}$$

$$|\xi_{ij,s}| \leq M^\Theta(1-w_{ij}^{SW}) \tag{9}$$

$$\forall ij \in \Gamma_B, s \in \Gamma_S$$

Constraints (2) and (3) are the active and reactive power balance constraints, respectively, representing the application of Kirchhoff's current law to the system. Note that, loads are modeled in this formulation through the voltage-dependent ZIP load model [14]. Constraint (4) calculates the voltage magnitude at a node from the value of the squared voltage magnitude using a Taylor's series expansion of the square root of $V_{i,s}^{SQ}$ at $(\overline{V}+\underline{V})/2$. Constraints (5)–(9) represent the systematic application of Kirchhoff's voltage law to the system, in which (8) and (9) are used to calculate the slack variables $\zeta_{ij,t,}$ and $\xi_{ij,t,s}$ according with the statuses of the switches. Constraint (7) is a second-order cone constraint, that must be active at the problem's solution.

C. Physical and Operational Limits of the System

Constraints (10)–(14) are the physical and operational limits of the system.

$$0 \leq I_{ij,s}^{SQ} \leq \overline{I}_{ij}^2 w_{ij}^{SW} \qquad \forall ij \in \Gamma_B, s \in \Gamma_S \tag{10}$$

$$|P_{ij,s}| \leq \overline{VI}_{ij} w_{ij}^{SW} \qquad \forall ij \in \Gamma_B, s \in \Gamma_S \tag{11}$$

$$|Q_{ij,s}| \leq \overline{VI}_{ij} w_{ij}^{SW} \qquad \forall ij \in \Gamma_B, s \in \Gamma_S \tag{12}$$

$$\underline{V}^2 \leq V_{i,s}^{SQ} \leq \overline{V}^2 \qquad \forall i \in \Gamma_N, s \in \Gamma_S \tag{13}$$

$$(P_{i,s}^{SS})^2 + (Q_{i,s}^{SS})^2 \leq \left(\overline{S}_i^{SS}\right)^2 \qquad \forall i \in \Gamma_{SS}, s \in \Gamma_S \tag{14}$$

According to the switch status, constraints (10)–(12) define the current capacity, active, and reactive limits for the branches, (13) is the voltage limit for the nodes, and (14) is the apparent power capacity of the SSs.

D. Operation of the SSs' OLTCs and VRs

The operation of SSs' OLTCs and VRs can be modeled considering integer tap steps. However, an integer representation increases the complexity of the problem. Therefore, a continuous formulation of the tap of SSs' OLTCs and VRs is used in this paper.

Consider an ideal transformer with a tap ratio $1:\Delta_{ij}^{TC}+1$ in series with the transformer impedance $R_{ij}+jX_{ij}$, presented in Fig. 1. The calculation of the square of the voltage magnitude at node k is shown in (15), while (16) defines δ_{ij}^{TC}, the difference between the square of the voltage magnitudes at nodes k and i.

$$V_k^2 = (\Delta_{ij}^{TC}+1)^2 V_i^2 \tag{15}$$

$$\delta_{ij}^{TC} = V_k^2 - V_i^2 = \Delta_{ij}^{TC}(\Delta_{ij}^{TC}+2)V_i^2 \tag{16}$$

Equation (17) shows how to obtain the value of the tap from δ_{ij}^{TC} and V_i.

$$\Delta_{ij}^{TC}+1 = \frac{\sqrt{V_i^2+\delta_{ij}^{TC}}}{V_i} \tag{17}$$

Based on these considerations, the operation of the SSs' OLTCs and VRs is modeled in (18) [11].

$$|\delta_{ij,s}^{TC}| \leq \overline{\Delta}_{ij}^{TC}(\overline{\Delta}_{ij}^{TC}+2)V_{i,s}^{SQ} \qquad \forall ij \in \Gamma_{TC}, s \in \Gamma_S \tag{18}$$

Constraint (18) calculates $\delta_{ij,s}^{TC}$ considering the voltage $V_{i,s}^{SQ}$ and $\overline{\Delta}_{ij}^{TC}$.

E. Operation of CBs

The operation of the CBs is formulated using a voltage-dependent model, as presented in (19)–(21).

$$\hat{Q}_{i,s}^{CB} = \sum_{k=1}^{\overline{n}_i^{CB}} Q_{i,k,s}^{CB} \qquad \forall i \in \Gamma_{CB}, s \in \Gamma_S \tag{19}$$

$$-B_i^{CB}\overline{V}^2(1-y_{i,k,s}^{CB}) \leq Q_{i,k,s}^{CB} - B_i^{CB}V_{i,s}^{SQ} \leq -B_i^{CB}\underline{V}^2(1-y_{i,k,s}^{CB}) \tag{20}$$

$$B_i^{CB}\underline{V}^2 y_{i,k,s}^{CB} \leq Q_{i,k,s}^{CB} \leq B_i^{CB}\overline{V}^2 y_{i,k,s}^{CB} \tag{21}$$

$$\forall i \in \Gamma_{CB}, k \in \{1,\cdots,\overline{n}_{ij}^{CB}\}, s \in \Gamma_S$$

Constraint (19) calculates the total reactive power injected by a CB at a node, while (20) and (21) calculate the reactive power injected by each CB module. Note that, if $y_{i,k,s}^{CB}=0$, then $Q_{i,k,s}^{CB}=0$ in (21). On the other hand, if $y_{i,k,s}^{CB}=1$, then $Q_{i,k,s}^{CB} = B_i^{CB}V_{i,s}^{SQ}$ in (20).

F. Dispatchable DGs

The capacities of the dispatchable DGs are considered in (22)–(24).

$$(P_{i,s}^{DG})^2 + (Q_{i,s}^{DG})^2 \leq \left(\overline{S}_i^{DG}\right)^2 \qquad \forall i \in \Gamma_{DG}, s \in \Gamma_S \tag{22}$$

$$P_{i,s}^{DG} \geq 0 \qquad \forall i \in \Gamma_{DG}, s \in \Gamma_S \tag{23}$$

$$-P_{i,s}^{DG}\tan(\cos^{-1}(\underline{PF}_i^{DG})) \leq Q_{i,s}^{DG} \leq P_{i,s}^{DG}\tan(\cos^{-1}(\overline{PF}_i^{DG})) \tag{24}$$

$$\forall i \in \Gamma_{DG}, s \in \Gamma_S$$

Constraint (22) is the apparent power generation capacity of the DGs, (23) requires that a DG can only inject active power into the system, and (24) is the power factor limit for the DGs.

G. Topological Constraints

The connectivity of the system and the maximum number of loops allowed to be formed is controlled by (25)–(28) through fictitious demands that must be attended at all nodes.

$$|\Gamma_N| - |\Gamma_{SS}| \leq \sum_{ij\in\Gamma_B} w_{ij}^{SW} \leq |\Gamma_N| - |\Gamma_{SS}| + N^{LP} \tag{25}$$

$$\sum_{ji\in\Gamma_B} f_{ji} - \sum_{ij\in\Gamma_B} f_{ij} + g_i = 1 \qquad \forall i \in \Gamma_N \tag{26}$$

$$|f_{ij}| \leq |\Gamma_N| w_{ij}^{SW} \qquad \forall ij \in \Gamma_B \tag{27}$$

$$0 \leq g_i \leq |\Gamma_N| \qquad \forall i \in \Gamma_{SS} \tag{28}$$

Constraint (25) controls the maximum number of basic loops in the system together with (26)–(28), that ensure the connectivity of the system, i.e., that there must be a path from

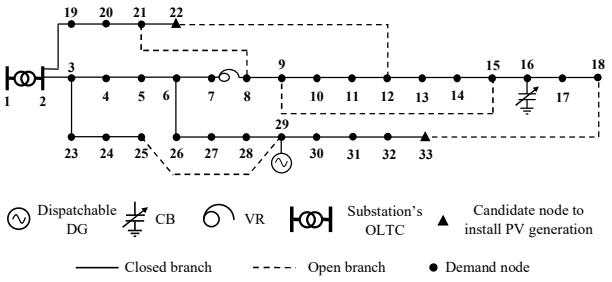

Fig. 2 Initial configuration of the 33-node system.

each node of the system to a SS. For the load nodes ($\{\Gamma_N - \Gamma_{SS}\}$), $g_i = 0$.

H. PV Hosting Capacity

The PV hosting capacity model is described in (29)–(32). Equation (33) calculates the total emissions from the system.

$$P_{i,s}^{PV} = \lambda_{i,s}^{PV} \overline{P}_i^{PV} - P_{i,s}^{C} \qquad \forall i \in \Gamma_{PV}, s \in \Gamma_S \tag{29}$$

$$0 \leq P_{i,s}^{C} \leq \lambda_{i,s}^{PV} \overline{P}_i^{PV} \qquad \forall i \in \Gamma_{PV}, s \in \Gamma_S \tag{30}$$

$$-P_{i,s}^{PV} \tan(\cos^{-1}(\underline{PF}_i^{PV})) \leq Q_{i,s}^{PV} \leq P_{i,s}^{PV} \tan(\cos^{-1}(\overline{PF}_i^{PV})) \qquad \forall i \in \Gamma_{PV}, s \in \Gamma_S \tag{31}$$

$$\sum_{s \in \Gamma_S} \Delta_s^T P_{i,s}^{C} \leq \psi_i \sum_{s \in \Gamma_S} \Delta_s^T \lambda_{i,s}^{PV} \overline{P}_i^{PV} \qquad \forall i \in \Gamma_{PV} \tag{32}$$

$$\xi = \sum_{i \in \Gamma_N} \sum_{s \in \Gamma_S} \Delta_s^T (e_{i,s}^{SS} P_{i,s}^{SS} + e_{i,s}^{DG} P_{i,s}^{DG}) \tag{33}$$

Constraint (29) determines the active power injected by the PV unit at node i according to the scenario, the installed capacity, and the active power curtailment. The power curtailment is determined in (30). The reactive power injected by the PV unit is limited in (31). The total power curtailment is limited according to (32). Finally, the total CO_2 emissions from the system is calculated in (33).

In the proposed formulation, the objective function (1) is linear, as well constraints (2)–(6), (8)–(14), (18)–(21), and (23)–(32). Constraint (7) is a second-order cone, while (22) is a quadratic constraint. Due to the presence of the binary variables w_{ij}^{SW} and $y_{i,k,s}^{CB}$, the resulting formulation is an MISOCP model, which can be solved by off-the-shelf optimization solvers.

III. Tests and Results

The proposed model is tested using the 33-node system shown in Fig. 2, which operates at 12.66 kV. This system has a 250 kVA dispatchable DG at node 29 with $\underline{PF}_i^{DG} = \overline{PF}_i^{DG} = 0.8$ and $e_{i,s}^{DG} = 0.63$ kg CO_2/kWh. A switchable CB with two modules of 150 kVAr is installed at node 16. A VR is installed at branch 7–8, with a maximum regulation of 10% and ±16 positions, while the OLTC at the SS has ±16 positions with a maximum regulation of 5%. Nodes 22 and 33 are candidates for the installation of PV generation, for which $\underline{PF}_i^{PV} = 0.95$ and $\overline{PF}_i^{PV} = 0.90$, and the maximum curtailment allowed is $\psi_i = 10\%$. For the substation, $e_{i,s}^{DG} = 2.17$ kg CO_2/kWh. The maximum and minimum voltage limits are 1.05 p.u. and 0.95 p.u., respectively.

A planning horizon of one year is considered. To represent the load behavior and solar irradiation, historical data of the seasons are obtained from [15] and the *k*-means clustering technique is used to reduce it to a suitable set of 24 scenarios using the procedure described in [2].

The proposed formulation was implemented in AMPL [16] and solved with the commercial solver CPLEX v20.1.0 [17] on a computer with a 3.2 GHz Intel® Core™ i7–8700 processor and 32 GB of RAM. Complete data for the 33-node system is available in [18].

A. Study Cases

The maximization of the PV hosting capacity of the system is analyzed considering the following four cases:

I. Without considering network reconfiguration (the closed branches of the initial configuration of the system cannot be opened) and without considering voltage control (the adjustments of the SS's OLTC, VR, and CB are fixed at their initial states)—as proposed in [12];

II. Without considering network reconfiguration and considering voltage control (optimizing the operation of the SS's OLTC, VR, and CB)—this proposal is presented in [13] only for radial configurations;

III. Considering network reconfiguration and without considering voltage control;

IV. Considering both network reconfiguration and voltage control—as proposed in this paper;

In all cases, it is considered the closed-loop operation of the system.

B. Discussion of the Results

Tables I–IV present the total hosting capacities for PV generation in the 33-node system obtained for Cases I–IV, respectively. These tables also provide the maximum capacities for PV generation integration at nodes 22 and 33, the configurations of the network, represented by the open branches, and information on the expected values of CO_2 emissions for each case.

By analyzing Table I, it can be verified that the maximum value of PV generation that can be integrated into the 33-node system is 5,947.36 kW considering the initial topology of the network without performing voltage control. It can be also verified that the maximum penetration of PV generation can be increased by a further 68.71%, to 10,033.56 kW, by only closing branch 12-22, therefore forming one loop in the network. Moreover, by closing more branches, the maximum penetration of PV generation can be increased up to 4.69%, to 10,504.21 kW, when all branches are closed.

By considering voltage control, Table II shows that the maximum penetration of PV generation can be increased by another 38.79%, to 8,254.36 kW, in relation to the initial radial configuration. By closing branch 12-22, the PV penetration can be increased by a further 23.26%, to 10,174.00 kW. The maximum PV penetration that can be achieved in this case is 10,530.28 kW, which represents an increase of 3.50% in relation to the solution with one loop.

By performing network reconfiguration, without voltage control (see Table III), the PV penetration can be increased by another 71.92%, to 10,224.64 kW, in relation to the initial radial configuration. Note that this solution presents a hosting capacity for PV generation 0.50% higher than the solution obtained for Case II when one loop is allowed in the system. Moreover, in this case, by allowing closed-loop topologies, the PV penetrations can be increased up to 2.73%, to 10,504.21 kW, when all branches are closed.

TABLE I

RESULTS FOR THE 33-NODE SYSTEM – CASE I: WITHOUT CONSIDERING NETWORK RECONFIGURATION AND VOLTAGE CONTROL

Results	Radial	1 Loop	2 Loops	3 Loops	4 Loops	5 Loops
Total PV generation installed (kW)	5,947.36	10,033.56	10,243.76	10,366.62	10,470.46	10,504.21
PV generation installed at nodes 22/33 (kW)	1,815.42/4,131.94	5,948.31/4,085.25	3,833.30/6,410.45	3,974.40/6,392.21	3,484.96/6,985.50	4,479.78/6,024.43
Open switches	8-21, 9-15, 12-22, 18-33, 25-29	8-21, 9-15, 18-33, 25-29	8-21, 9-15, 25-29	9-15, 25-29	25-29	–
Emissions from the main grid (tonnes)	59,260.18	47,353.86	46,907.22	47,029.09	46,975.92	46,886.86
Emissions from the DG (tonnes)	1,016.79	793.18	853.53	796.39	792.82	796.27
Total emissions (tonnes)	60,276.98	48,147.04	47,760.75	47,825.48	47,768.74	47,683.13

TABLE II

RESULTS FOR THE 33-NODE SYSTEM – CASE II: WITHOUT CONSIDERING NETWORK RECONFIGURATION AND CONSIDERING VOLTAGE CONTROL

Results	Radial	1 Loop	2 Loops	3 Loops	4 Loops	5 Loops
Total PV generation installed (kW)	8,254.36	10,174.00	10,318.03	10,422.54	10,491.57	10,530.28
PV generation installed at nodes 22/33 (kW)	4,209.21/4,045.15	6,087.87/4,086.13	6,345.10/3,972.94	6,449.42/3,973.12	3,594.85/6,896.72	3,942.03/6,588.25
Open switches	8-21, 9-15, 12-22, 18-33, 25-29	8-21, 9-15, 18-33, 25-29	9-15, 18-33, 25-29	18-33, 25-29	25-29	–
Emissions from the main grid (tonnes)	45,580.13	46,452.71	45,607.38	45,484.46	45,426.47	41,181.94
Emissions from the DG (tonnes)	1,193.61	614.61	804.69	797.51	788.06	840.54
Total emissions (tonnes)	46,773.74	47,067.32	46,412.07	46,281.97	46,214.53	42,022.48

TABLE III

RESULTS FOR THE 33-NODE SYSTEM – CASE III: CONSIDERING NETWORK RECONFIGURATION AND NOT CONSIDERING VOLTAGE CONTROL

Results	Radial	1 Loop	2 Loops	3 Loops	4 Loops	5 Loops
Total PV generation installed (kW)	10,224.64	10,396.16	10,426.75	10,457.46	10,490.64	10,504.21
PV generation installed at nodes 22/33 (kW)	5,536.47/4,688.17	4,087.32/6,308.83	3,829.94/6,596.81	3,516.82/6,940.63	4,529.65/5,961.00	4,479.78/6,024.43
Open switches	6-7, 14-15, 15-16, 8-21, 25-29	6-7, 10-11, 14-15, 25-29	10-11, 14-15, 25-29	10-11, 25-29	10-11	–
Emissions from the main grid (tonnes)	46,855.22	46,852.33	46,958.45	46,932.86	46,892.29	46,886.86
Emissions from the DG (tonnes)	807.86	823.60	807.85	809.06	799.56	796.27
Total emissions (tonnes)	47,663.07	47,675.93	47,766.30	47741.92	47,691.85	47,683.13

TABLE IV

RESULTS FOR THE 33-NODE SYSTEM – CASE IV: CONSIDERING BOTH NETWORK RECONFIGURATION AND VOLTAGE CONTROL

Results	Radial	1 Loop	2 Loops	3 Loops	4 Loops	5 Loops
Total PV generation installed (kW)	10,262.46	10,428.75	10,437.92	10,484.10	10,512.72	10,530.28
PV generation installed at nodes 22/33 (kW)	5,550.09/4,712.37	4,181.86/6,246.90	3,738.27/6,699.65	3,974.24/6,509.86	3,924.21/6,588.51	3,942.03/6,588.25
Open switches	6-7, 8-9, 10-11, 15-16, 25-29	6-7, 10-11, 14-15, 25-29	10-11, 14-15, 28-29	10-11, 14-15	10-11	–
Emissions from the main grid (tonnes)	42,464.53	42,007.52	41,608.38	41,312.00	41,373.60	41,181.94
Emissions from the DG (tonnes)	807.65	793.46	829.96	819.45	794.51	840.54
Total emissions (tonnes)	43,272.19	42,800.98	42,438.33	42,131.45	42,168.12	42,022.48

Finally, by analyzing Table IV, it is possible to verify that the penetration of PV generation can be increased by a further 72.55%, to 10,262.46 kW, in relation to the initial radial configuration. By allowing the formation of more loops in the system, the PV penetration can be increased by more 2.61%, up to 10,530.28 kW.

Therefore, it can be verified that network reconfiguration with simultaneous voltage control can provide more flexible solutions to the problem. For example, the solution with only one loop obtained in Case IV has a maximum PV hosting capacity that is 0.06% higher than the solution with three loops of Case II. Since the formation of many loops may bring problems to the system operation [11], the proposed approach can provide more suitable solutions to the problem.

The computational times to solve all cases are always lower than four minutes. All the obtained solutions were evaluated with a power flow algorithm, in order to verify the operational limits of the network.

IV. Conclusions

This paper presented a novel stochastic mixed-integer second-order cone programming model for the problem of short-term planning of active distribution systems for increasing the photovoltaic (PV) generation hosting capacity of the network. The operational actions included voltage control and network reconfiguration.

Voltage control was considered through the optimal adjustment of capacitors banks, substations' on-load tap changers, and voltage regulators. Besides that, the formulation considered network reconfiguration with both radial and closed-loop operation.

The obtained results showed a higher capacity for PV generation penetration and CO_2 emissions mitigation when voltage control and reconfiguration with closed-loop topologies were considered. Moreover, it was demonstrated that more flexibility is achieved when both reconfiguration allowing closed-loop operation and voltage control are considered simultaneously in the problem. Thus, the alternative of performing voltage control and network reconfiguration allowing closed-loop topologies in active distribution systems can provide more environmentally friendly and efficient operation schemes postponing the necessity of investments for reinforcing the network structure.

Acknowledgment

This work was supported by the Coordination for the Improvement of Higher Education Personnel (CAPES) – Finance Code 001, the Brazilian National Council for Scientific and Technological Development (CNPq), grants 305852/2017-5 and 304726/2020-6, the São Paulo Research Foundation (FAPESP), under grants 2015/21972-6, 2018/20355-1, 2019/19632-3, 2019/01841-5, and 2019/23755-3, and by ENEL under the grant PEE-00390-1062/2017 - P&D-00390-1083-2020_UFABC, ANEEL 001-2016.

References

[1] A. Ferreira *et al.*, "Economic overview of the use and production of photovoltaic solar energy in Brazil," *Renew. Sustain. Energy Rev.*, vol. 81, pp. 181–191, Jan. 2018.

[2] J. M. Home-Ortiz, M. Pourakbari-Kasmaei, M. Lehtonen, and J. R. Sanches Mantovani, "Optimal location-allocation of storage devices and renewable-based DG in distribution systems," *Electr. Power Syst. Res.*, vol. 172, pp. 11–21, Jul. 2019.

[3] M. U. Hashmi, D. Deka, A. Busic, L. Pereira, and S. Backhaus, "Arbitrage with power factor correction using energy storage," *IEEE Trans. Power Syst.*, vol. 35, no. 4, pp. 2693–2703, Jul. 2020.

[4] R. Mahat, K. Duwadi, F. B. dos Reis, R. Fourney, R. Tonkoski, and T. M. Hansen, "Techno-economic analysis of PV inverter controllers for preventing overvoltage in LV grids," in *2020 International Symposium on Power Electronics, Electrical Drives, Automation and Motion (SPEEDAM)*, 2020, pp. 502–507.

[5] S. F. Santos, D. Z. Fitiwi, M. Shafie-Khah, A. W. Bizuayehu, C. M. P. Cabrita, and J. P. S. Catalão, "New multistage and stochastic mathematical model for maximizing RES hosting capacity—Part I: problem formulation," *IEEE Trans. Sustain. Energy*, vol. 8, no. 1, pp. 304–319, Jan. 2017.

[6] S. F. Santos, D. Z. Fitiwi, M. Shafie-Khah, A. W. Bizuayehu, C. M. P. Cabrita, and J. P. S. Catalão, "New multi-stage and stochastic mathematical model for maximizing RES hosting capacity—Part II: numerical results," *IEEE Trans. Sustain. Energy*, vol. 8, no. 1, pp. 320–330, Jan. 2017.

[7] F. Capitanescu, L. F. Ochoa, H. Margossian, and N. D. Hatziargyriou, "Assessing the potential of network reconfiguration to improve distributed generation hosting capacity in active distribution systems," *IEEE Trans. Power Syst.*, vol. 30, no. 1, pp. 346–356, Jan. 2015.

[8] R. A. Jacob and J. Zhang, "Distribution network reconfiguration to increase photovoltaic hosting capacity," in *2020 IEEE Power & Energy Society General Meeting (PESGM)*, 2020, pp. 1–5.

[9] D. Ritter, J. F. Franco, and R. Romero, "Analysis of the radial operation of distribution systems considering operation with minimal losses," *Int. J. Electr. Power Energy Syst.*, vol. 67, pp. 453–461, May 2015.

[10] T.-H. Chen, W.-T. Huang, J.-C. Gu, G.-C. Pu, Y.-F. Hsu, and T.-Y. Guo, "Feasibility study of upgrading primary feeders from radial and open-loop to normally closed-loop arrangement," *IEEE Trans. Power Syst.*, vol. 19, no. 3, pp. 1308–1316, Aug. 2004.

[11] R. Vargas, L. H. Macedo, J. M. Home-Ortiz, J. R. S. Mantovani, and R. Romero, "Optimal restoration of active distribution systems with voltage control and closed-loop operation," *IEEE Trans. Smart Grid*, pp. 1–1, Jan. 2021.

[12] M. R. M. Cruz, D. Z. Fitiwi, S. F. Santos, S. J. P. S. Mariano, and J. P. S. Catalão, "Prospects of a meshed electrical distribution system featuring large-scale variable renewable power," *Energies*, vol. 11, no. 12, Dec. 2018.

[13] D. A. Quijano, J. Wang, M. R. Sarker, and A. Padilha-Feltrin, "Stochastic assessment of distributed generation hosting capacity and energy efficiency in active distribution networks," *IET Gener. Transm. Distrib.*, vol. 11, no. 18, pp. 4617–4625, Dec. 2017.

[14] L. M. Hajagos and B. Danai, "Laboratory measurements and models of modern loads and their effect on voltage stability studies," *IEEE Trans. Power Syst.*, vol. 13, no. 2, pp. 584–592, May 1998.

[15] S. Pfenninger and I. Staffell, "Renewables.ninja," 2020. [Online]. Available: https://www.renewables.ninja/. [Accessed: 01-Nov-2020].

[16] R. Fourer, D. M. Gay, and B. W. Kernighan, *AMPL: a modeling language for mathematical programming*, 2nd ed. Duxbury, MA, USA: Thomson, 2003.

[17] IBM, "IBM ILOG CPLEX Optimization Studio 20.1.0 documentation," *2021*. [Online]. Available: https://www.ibm.com/support/knowledgecenter/SSSA5P_20.1.0/COS_KC_home.html. [Accessed: 01-Feb-2021].

[18] "LaPSEE power system test cases repository," 2021. [Online]. Available: http://www.feis.unesp.br/#!/lapsee. [Accessed: 01-Feb-2021].